

The infrared spectrum of NNCO^+ trapped in solid neon

Warren E. Thompson^{a)} and Marilyn E. Jacox^{b)}

Sensor Science Division, National Institute of Standards and Technology, Gaithersburg, Maryland 20899-8441, USA

(Received 14 October 2011; accepted 3 November 2011; published online 13 December 2011)

Codeposition of a $\text{Ne:N}_2:\text{CO} = 200:1:1$ mixture at 4.3 K with a beam of very pure neon atoms excited to their energy levels between 16.6 and 16.85 eV leads to stabilization in the resulting solid of sufficient NNCO^+ for detection of its NN- and CO-stretching vibration fundamentals. Detailed isotopic substitution studies and density functional calculations for the various isotopologues support the identification of NNCO^+ and permit estimation of the positions of two of its low-frequency fundamentals. A sufficient concentration of NOCN is also stabilized in the neon matrix for detection of its NO-stretching vibrational fundamental. [doi:10.1063/1.3666046]

I. INTRODUCTION

Compounds formed by the combination of N_2 and CO are of fundamental interest and have been proposed as high energy density materials and as components of planetary ices. Despite the ubiquity of both parent molecules, much remains to be learned about the products of their reaction.

The first such species to be detected was nitrosyl cyanide, NCNO , tentatively identified by Horsewood and Kirby¹ in 1971 and shortly thereafter confirmed by detailed microwave studies.² In 1997, Maier *et al.*³ obtained the infrared spectra of NCNO and of the two chain structures which contain a nitrosyl group and are next higher in energy— CNNO and NOCN —trapped in an argon matrix. However, the most stable N_2CO species was calculated⁴ to be diazirinone, cyclic $(\text{N}_2\text{C}) = \text{O}$. In 2005, neutralization-reionization experiments⁵ demonstrated that an uncharged N_2CO species in which the N_2 and CO moieties are linked is stable, but only very recently has such a species been observed. Experiments in the laboratory of Beckers and Willner⁶ have provided a detailed assignment of the infrared spectra of diazirinone and of several of its isotopologues trapped in neon and argon matrices. Their observed values for the vibrational fundamentals of diazirinone are in excellent agreement with the values predicted by *ab initio* and density functional calculations. They have also reported⁷ a high-resolution gas-phase study of the ν_1 and $2\nu_5$ bands of this species, providing definitive proof of its C_{2v} ring structure.

The evidence for the existence of stable uncharged N_2CO obtained by de Petris *et al.*⁵ depended on the existence of a stable N_2CO^+ species, which had been established for sometime. Various workers have suggested that N_2CO^+ may participate in the chemistry of the upper atmosphere, interstellar clouds, cometary comae, planetary atmospheres, and combustion. Early evidence for it came from a study⁸ of charge transfer between N^+ and CO, with detection by laser-induced fluorescence of the CO^+ product. The relaxation of CO^+ ($v = 1$) by N_2 was unusually efficient, requiring only 6 or

7 collisions. A selected ion flow tube (SIFT) study of the interaction of CO^+ with N_2 by Ferguson *et al.*⁹ yielded a very large three-body association rate for these two species in the presence of helium. A later SIFT study¹⁰ found a reaction rate constant consistent with that of the earlier study and yielded a branching ratio of 1.0 for the formation of N_2CO^+ . Furthermore, Glosik *et al.*¹¹ obtained a bond energy of 0.7 ± 0.2 eV. A guided ion-beam study¹² of seven dissociative reaction channels each for the $\text{CO}^+ + \text{N}_2$ and the $\text{N}_2^+ + \text{CO}$ reactions suggested that all of these channels proceed through a common N_2CO^+ intermediate.

The only previous spectroscopic study of N_2CO^+ was that by Knight *et al.*,¹³ who obtained the electron spin resonance (ESR) spectrum of N_2CO^+ trapped in a neon matrix. They deduced a planar structure, bent on the oxygen end, with the *s* vs. *p* hybridization ratio on the C atom intermediate between the ratio for one of the central atoms of OCCO^+ and that for N_4^+ .

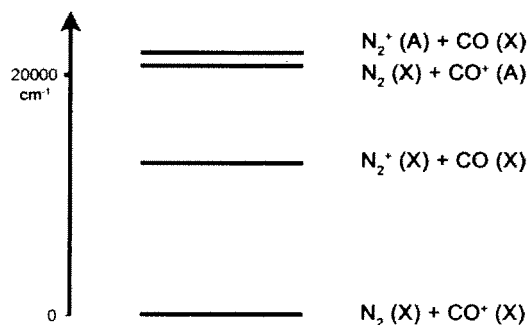
An early *ab initio* study of N_2CO^+ by Baker and Buckingham¹⁴ indicated that it was bound by about 1 eV, consistent with the SIFT observations. More recently, Hochlaf *et al.*¹⁵ conducted a detailed RCCSD(T)/cc-pVTZ study of the ground state of N_2CO^+ , using a variational procedure to evaluate the six fundamental vibrational frequencies. Anharmonic values for these frequencies were also obtained. High-level calculations gave a dissociation energy of 1.00 eV for the complex, consistent with the value obtained in the earlier studies. A planar *trans*-equilibrium structure was obtained, with charge transfer between N_2 and CO^+ .

As is shown in Figure 1, derived using the spectroscopic data summarized by Huber and Herzberg,¹⁶ the four lowest dissociation energies of NNCO^+ span an energy range of $\sim 22\,000$ cm^{-1} . Hochlaf¹⁷ has discussed the role of the related low-lying excited electronic states of N_2CO^+ in its formation and decomposition. Vibronic interactions and conical intersections of several of these states are important.

Experiments in this laboratory have led to the stabilization of a number of small molecular ions in concentration sufficient for infrared identification.¹⁸ Among these ions are N_4^+ (Ref. 19) and OCCO^+ ,²⁰ which are isoelectronic with

^{a)}Guest researcher.

^{b)}Electronic mail: marilyn.jacox@nist.gov.

FIG. 1. Low-lying dissociation limits of $\text{NN}\cdot\text{CO}^+$.

N_2CO^+ . Using a similar sampling procedure but much more sensitive ESR detection, Knight *et al.* had previously studied both N_4^+ (Ref. 21) and OCCO^+ .²² The success of that group in detecting the ESR spectrum of NNCO^+ (Ref. 13) adds to the promise of the corresponding infrared experiments.

II. EXPERIMENTAL DETAILS

The N_2 and CO used for these experiments were the same as those used for the earlier studies. Samples of each of these with a large excess of very pure neon (Spectra Gases, Inc., Research Grade, 99.999%) (Ref. 23) were mixed in a single bulb, using standard manometric procedures. All but one of the normal and isotopically enriched gas mixtures used in these experiments had a $\text{Ne}:\text{N}_2:\text{CO}$ mole ratio of 200:1:1. (The remaining mixture had a mole ratio of 300:3:1.)

The sample mixtures were codeposited at 4.3 K with a similar amount of pure neon that had been excited by a microwave discharge before streaming through a 1 mm pinhole in the end of a quartz discharge tube. Details of the deposition procedure and of the discharge configuration have been described previously.^{24,25} (The Nanochem filter was omitted in this series of experiments.)

The absorption spectra of the sample deposits were obtained using a Bomem DA 3.002 Fourier-transform interferometer with transfer optics that have been described previously.²⁶ All of the observations were conducted at a resolution of 0.2 cm^{-1} between 450 and 5000 cm^{-1} using a globar source, a KBr beamsplitter, and a wideband HgCdTe detector cooled to 77 K. Data were accumulated for each spectrum over a period of at least 15 min. The resulting spectrum was ratioed against a similar one taken without a deposit on the cryogenic mirror. Under these conditions, the positions of the prominent, nonblended atmospheric water vapor lines between 1385 and 1900 cm^{-1} and between 3620 and 3900 cm^{-1} , observed in a calibration scan, agreed to within 0.01 cm^{-1} with the high-resolution values reported by Toth.^{27,28} Based on previous investigations, with this experimental configuration the standard uncertainty (type B) in the determination of the absorption maxima for molecules trapped in solid neon is $\pm 0.1\text{ cm}^{-1}$ (coverage factor, $k = 1$, i.e., 1σ).

Information on photoinduced changes in the matrix sample was obtained by exposing the deposit to various wavelength ranges of near infrared, visible, and ultraviolet radiation. A tungsten background source was used with a filter of

Schott glass type RG1000, RG850, RG780, or RG695 or of Corning glass type 2404, 2424, or 3484 to exclude radiation of wavelength shorter than 1000, 850, 780, 695, 620, 580, or 520 nm, respectively. Irradiations were also conducted using a medium-pressure mercury arc source with a filter of Corning glass type 3384, 3389, or 7380 to exclude radiation of wavelength shorter than 490, 420, or 345 nm, respectively. Irradiations were also conducted using unfiltered medium-pressure arc emission, estimated to have a cutoff wavelength near 240 nm.

III. RESULTS AND DISCUSSION

A. Infrared spectrum of NNCO^+

In all of the experiments, the infrared spectra of the initial deposits included prominent product absorptions obtained in the corresponding experiments on $\text{Ne}:\text{N}_2$ samples¹⁹ and on $\text{Ne}:\text{CO}$ samples,²⁰ and assigned to the NN- and CO-stretching absorptions of various species. The positions of the cation product absorptions observed in these two earlier studies, together with those of N_2 , N_2^+ , CO , and CO^+ given by Huber and Herzberg,¹⁶ are summarized in Table I. The totally symmetric, infrared inactive NN- and CO-stretching fundamentals of N_4^+ and OCCO^+ are enclosed in square brackets. New absorptions also appeared at 2285.3 and 2148.7 cm^{-1} in the present series of experiments. Like the absorptions in the same spectral region that were assigned to N_4^+ , OCCO^+ , and CO^+ in the two earlier neon-matrix studies, these absorptions were destroyed by irradiation of the deposit with visible light. Their observed positions and the positions—including the anharmonic corrections—calculated by Hochlaf *et al.*¹⁵ for the NN- and CO-stretching fundamentals of NNCO^+ are also given in Table I. These two new relatively weak absorptions are marked by filled circles in Figure 2, which include traces obtained after the initial deposit had been subjected to mercury-arc irradiation through filters with short wavelength cutoff at 490 and 420 nm. In another experiment, the deposit was successively irradiated using a tungsten lamp and filters with short wavelength cutoffs of 780, 695, 620, and 520 nm.

TABLE I. NN- and CO-stretching fundamentals (cm^{-1}) of species related to NNCO^+ .

Species		ν_{NN}	ν_{CO}
N_2	Gas ^a	2329.9	
N_2^+	Gas ^a	2174.6	
N_4^+	Ne matrix ^b	[2283], 2237.6	
CO	Gas ^a		2143.2
CO^+	Gas ^a		2183.9
	Ne matrix ^c		2194.4
OCCO^+	Ne matrix ^c		[2076], 2056.6
NNCO^+	RCCSD(T)/cc-pVTZ ^d	2287.2	2071.0
NNCO^+	Ne matrix ^c	2285.3	2148.7

^aReference 16.

^bReference 19.

^cReference 20.

^dCorrected for anharmonicity, Ref. 15.

^eThis work. Based on previous investigations, the standard uncertainty (type B) in the neon-matrix measurements is 0.1 cm^{-1} (1σ).

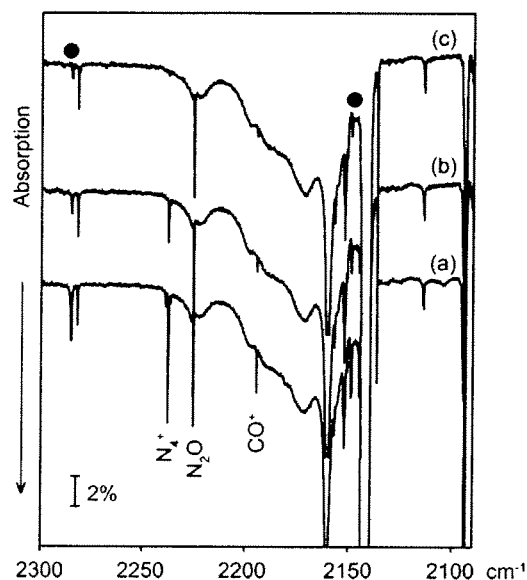


FIG. 2. Behavior of product absorptions between 2100 and 2300 cm^{-1} on sequential filtered mercury-arc irradiations: 10.30 mmol $\text{Ne:N}_2:\text{CO} = 200:1:1$ codeposited at 4.3 K over a period of 227 min with 10.11 mmol pure neon that had been passed through a microwave discharge. (a) Initial deposit; (b) 20-min Hg-arc irradiation, $\lambda > 490$ nm; and (c) 20-min Hg-arc irradiation, $\lambda > 420$ nm.

All three of the cation species named above and the carrier of the two new absorptions showed some evidence of photodestruction even when the 780 nm cutoff filter was used. Their photodestruction continued as the shorter wavelength cutoff filters were substituted. Such behavior is characteristic of cations isolated in solid neon. It has been attributed to photodetachment of electrons from various electron traps in the solid followed by migration of these electrons through the deposit, permitting cation-electron recombination. The phenomenon has been considered in more detail in a recent review.²⁹ The positions of the two new absorptions suggest their assignment to the NN- and CO-stretching vibrations of NNCO^+ .

Very weak absorptions which also were readily destroyed on irradiation of the deposit by visible light appeared at 2306.0, 2308.0, and 2309.2 cm^{-1} . An absorption near 2310 cm^{-1} by a readily photolyzed species has appeared in a number of experiments in which N_2 is present and ion production occurs. In all of the neon-matrix experiments, desorption of H_2O from the walls of the deposition system occurs during the several hours required for deposition of the sample. It has been proposed³⁰ that this absorption is contributed by a complex of N_2 with H_2O^+ .

Further information regarding the assignment of the two new absorptions which appear in the 2100–2300 cm^{-1} spectral region was obtained from a detailed study of their behavior on isotopic substitution.

Figure 3 shows the absorption pattern in the NN-stretching region (2200–2300 cm^{-1}) for several of the isotopically substituted sample mixtures. A thin vertical line has been drawn through the maximum of the NN-stretching absorption at 2285.3 cm^{-1} . A filled circle marks the counterpart of that peak in the isotopic enrichment experiments, and a

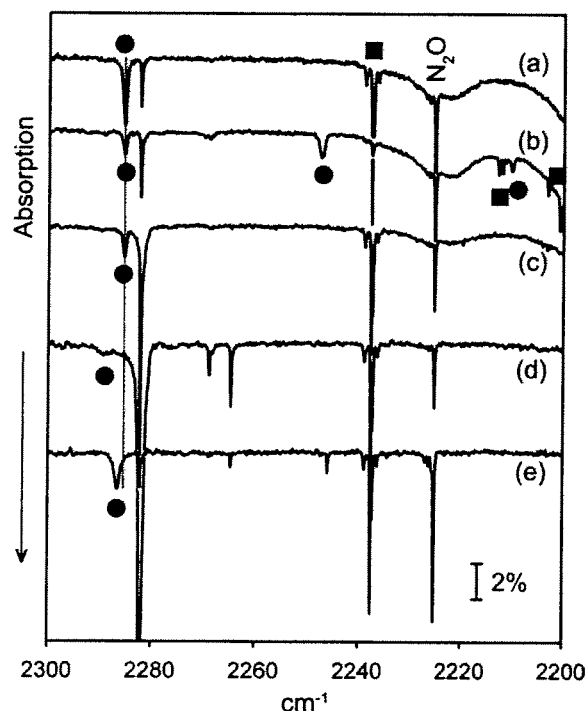


FIG. 3. Behavior of product absorptions between 2200 and 2300 cm^{-1} on isotopic enrichment of $\text{Ne:N}_2:\text{CO}$ samples: (a) 10.30 mmol $\text{Ne:N}_2:\text{CO} = 200:1:1$ codeposited at 4.3 K over a period of 227 min with 10.11 mmol pure neon that had been passed through a microwave discharge; (b) 10.94 mmol Ne:N_2 (47% ^{15}N): $\text{CO} = 200:1:1$ codeposited at 4.3 K over a period of 247 min with 11.83 mmol pure neon that had been passed through a microwave discharge; (c) 8.85 mmol $\text{Ne:N}_2:\text{CO}$ (52% ^{13}C) = 200:1:1 codeposited at 4.3 K over a period of 197 min with 9.91 mmol pure neon that had been passed through a microwave discharge; (d) 10.76 mmol $\text{Ne:N}_2:\text{CO}$ (93% ^{13}C) = 200:1:1 codeposited at 4.3 K over a period of 228 min with 10.71 mmol pure neon that had been passed through a microwave discharge; and (e) 8.94 mmol $\text{Ne:N}_2:\text{CO}$ (96% ^{18}O) = 200:1:1 codeposited at 4.3 K over a period of 200 min with 10.31 mmol pure neon that had been passed through a microwave discharge.

filled square marks other absorptions previously assigned¹⁹ to isotopologues of N_4^+ . Trace (a) is an expanded plot of the same data for the unenriched system as that shown in trace (a) of Figure 2. A prominent, very sharp absorption of ν_3 of CO_2 is present in all of the discharge sampling experiments. The unmarked peak near 2282 cm^{-1} is contributed by $^{13}\text{CO}_2$ present in natural abundance. Trace (b) of Figure 3 shows the observations in an experiment with 47% random enrichment of the N_2 in nitrogen-15. Three photosensitive absorptions appear at 2285.3, 2247.3, and 2210.1 cm^{-1} . This behavior indicates that the product contains two symmetrically equivalent N atoms and/or that the NN and CO moieties are only weakly coupled. Trace (c) shows the results of a study using 52% ^{13}CO enrichment. There is no shift in the 2285.3 cm^{-1} absorption, suggesting that the N_2 and CO moieties are weakly coupled. In this experiment, the absorption of $^{13}\text{CO}_2$ was more intense than in the experiment of trace (b). Trace (d) was obtained from an experiment with 93% ^{13}CO enrichment. There is no detectable absorption at 2285.3 cm^{-1} , but a weak, very broad, photosensitive absorption is centered at 2289.5 cm^{-1} . The $^{13}\text{CO}_2$ absorption near 2282 cm^{-1} is very prominent. The two new absorptions between 2260 and 2270 cm^{-1} persist on mercury-arc irradiation through the

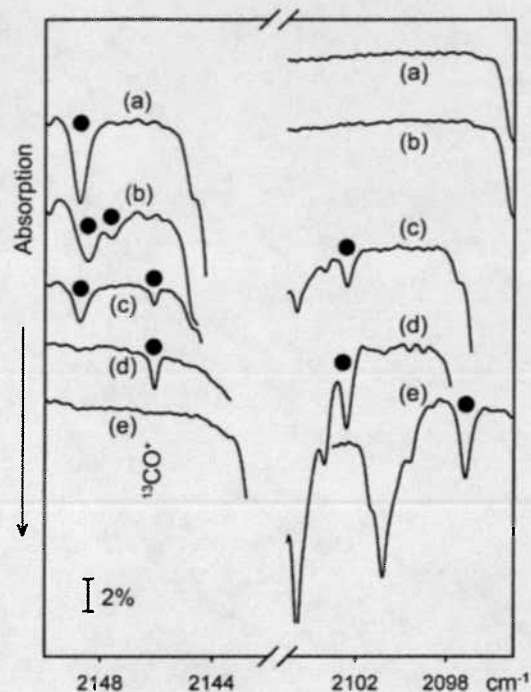


FIG. 4. Behavior of product absorptions between 2095 and 2150 cm^{-1} on isotopic enrichment of the same Ne:N₂:CO samples as those for which spectra are shown in Figure 3.

420-nm cutoff filter, indicating that they are not contributed by the product of interest. Fermi resonance between the NN-stretching fundamental of NN¹³CO⁺ and a combination band involving the CO-stretching fundamental of that species and a low-frequency fundamental could account for the unusual behavior in the NN-stretching region. Presumably, the other component of the Fermi resonance doublet is masked by the strong ¹³CO₂ absorption. Trace (e) shows the spectrum between 2200 and 2300 cm^{-1} for a sample in which the CO is enriched to 96% in C¹⁸O. A new, photosensitive absorption appears at 2286.5 cm^{-1} , 1.2 cm^{-1} above its counterpart for the unsubstituted product. The peak height for the ¹³CO₂ absorption is similar to that in trace (a), but in the figure is overlapped by the very prominent absorption near 2282 cm^{-1} of trace (d).

Figure 4 shows the CO-stretching region of the same isotopically enriched samples as those for which the NN-stretching region is shown in Figure 3. Filled circles designate peaks destroyed by exposing the deposit to visible light. Because the absorptions of ¹³CO and of C¹⁸O are very strong and are detectable in natural abundance even in unenriched CO samples, they are not shown in the plot. The only photosensitive absorption in trace (a) is that at 2148.7 cm^{-1} , attributed to unenriched NNCO⁺. The mixture of trace (b) was prepared using a nitrogen sample with 47% random enrichment in nitrogen-15. Two absorptions appear in the CO-stretching region. The more prominent one is a relatively broad peak with maximum at 2148.3 cm^{-1} , slightly below the 2148.7 cm^{-1} absorption of the unenriched complex. A less intense peak is partially resolved at 2147.6 cm^{-1} . Presumably the absorption of the unenriched complex is unresolved from that of the two singly nitrogen-15 enriched species and the lower

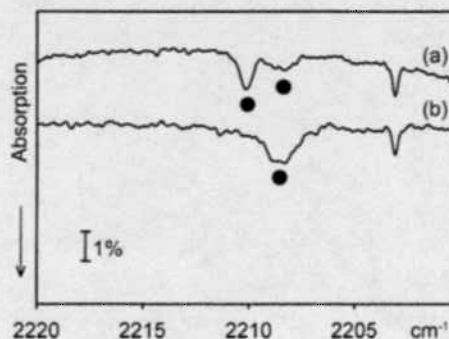


FIG. 5. Behavior of product absorptions between 2200 and 2220 cm^{-1} on carbon-13 enrichment of Ne:N₂:CO samples that are heavily enriched in nitrogen-15: (a) 8.73 mmol Ne:N₂ (97% ¹⁵N):CO (52% ¹³C) = 200:1:1 codeposited at 4.3 K over a period of 188 min with 9.15 mmol pure neon that had been passed through a microwave discharge and (b) 10.38 mmol Ne:N₂ (97% ¹⁵N):CO (93% ¹³C) = 200:1:1 codeposited at 4.3 K over a period of 221 min with 10.76 mmol pure neon that had been passed through a microwave discharge.

frequency shoulder is contributed by the doubly nitrogen-15 enriched product. Trace (c) was obtained for the sample with 52% enrichment in ¹³CO. A weak, photosensitive absorption at 2146.0 cm^{-1} is contributed by ¹³CO⁺, in agreement with the previously reported²⁰ position for the absorption of ¹³CO⁺ isolated in a neon matrix. (The absorption of unenriched CO⁺ appeared at 2194.4 cm^{-1} , outside the range of this plot.) Approximately equally intense absorptions at 2148.6 and 2102.2 cm^{-1} are attributed to NN¹²CO⁺ and NN¹³CO⁺, respectively. Trace (d) was obtained using a sample with 93% ¹³CO enrichment. The 2148.6 cm^{-1} peak is not present, but the 2146.0 cm^{-1} ¹³CO⁺ absorption and the 2102.2 cm^{-1} peak are enhanced in intensity. Trace (e) shows this spectral region for a sample enriched to 96% in C¹⁸O. As in the earlier study,²⁰ the anticipated neon-matrix absorption of C¹⁸O⁺ near 2142 cm^{-1} is obscured by the much stronger absorption of residual ¹²C¹⁶O. A new, photosensitive absorption appears at 2097.1 cm^{-1} .

Figure 5 shows the NN-stretching absorption pattern for samples prepared using heavy enrichment of the nitrogen sample in nitrogen-15 and two different extents of carbon-13 enrichment of the CO. Filled circles designate peaks destroyed by exposing the deposit to visible light. The sample used to obtain trace (a) had 52% enrichment in ¹³CO. The photosensitive 2210.1 cm^{-1} peak previously attributed to the product of the interaction of ¹⁵N₂ with ¹²CO predominates, with a weaker, relatively broad satellite at 2208.5 cm^{-1} . Trace (b) was obtained using a sample with 93% enrichment in ¹³CO. The only photosensitive absorption in the NN-stretching region is that at 2208.5 cm^{-1} . Once again, the breadth of this peak suggests a Fermi resonance interaction with a combination band.

Figure 6 shows the CO-stretching region for samples heavily enriched in nitrogen-15 and with partial and heavy enrichment in ¹³CO. Filled circles designate peaks destroyed by exposing the deposit to visible light. Trace (a) was obtained for a sample enriched to 52% in ¹³CO. As before, a weak photosensitive absorption of ¹³CO⁺ appears at 2146.0 cm^{-1} . More prominent photosensitive absorptions of approximately

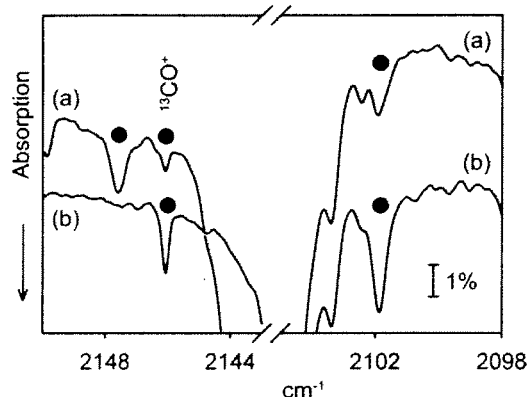


FIG. 6. Behavior of product absorptions between 2098 and 2150 cm^{-1} on carbon-13 enrichment of the same Ne: N_2 (97% ^{15}N):CO samples as those for which spectra are shown in Figure 5.

equal intensity appear at 2102.2 and 2147.6 cm^{-1} . In trace (b), obtained using 93% ^{13}C , the $^{13}\text{CO}^+$ absorption appears at 2146.0 cm^{-1} , together with a more prominent, photosensitive absorption at 2101.9 cm^{-1} , but no detectable absorption at 2147.6 cm^{-1} .

All of the experimental observations presented in Figures 3–6 are summarized in Table II.

Analysis of the isotopic substitution observations was facilitated by calculations of the isotopic substitution behavior of the vibrational fundamentals of NNCO⁺ using the

TABLE III. Calculated structure of NNCO⁺.

Coordinate	RCCSD(T)/cc-pVTZ ^a	UB3LYP/cc-pVTZ ^b
R_{NN} (Å)	1.106	1.094
R_{NC} (Å)	1.914	1.911
R_{CO} (Å)	1.127	1.116
$\angle \text{NNC}$	175.3°	161.3°
$\angle \text{NCO}$	129.1°	131.1°
τ (dihedral angle)	180°	180°

^aReference 15.

^bThis work.

GAUSSIAN 03 program package.³¹ The positions of the ground-state fundamentals were obtained by density functional calculations using the unrestricted B3LYP procedure³² together with the correlation-consistent polarized valence triple-zeta basis set (cc-pVTZ) developed by Dunning.³³

As is shown in Table III, our density functional calculation of the structure of NNCO⁺ agrees quite well with the planar, *trans*-bent structure obtained in the *ab initio* calculations of Hochlaf *et al.*¹⁵

The unscaled fundamental vibrational frequencies for NNCO⁺ and its isotopologues obtained in the density functional calculations are included in Table II. Calculated intensities are given in parentheses. Scaling factors were also applied to match the NN- and CO-stretching fundamental frequencies to those observed for the unenriched species. The resulting

TABLE II. Calculated^a and observed^b vibrational fundamentals (cm^{-1}) of isotopologues of NNCO⁺.

Species		ω_1, ν_1 (a')	ω_2, ν_2 (a')	ω_3, ν_3 (a')	ω_4, ν_4 (a')	ω_5, ν_5 (a')	ω_6, ν_6 (a'')
$^{14}\text{N}^{14}\text{N}^{12}\text{C}^{16}\text{O}^+$	RCCSD(T)/cc-pVTZ ^c (ω)	2316.8	2169.1	502.8	181.2	101.1	118.8
	RCCSD(T)/cc-pVTZ ^c (ν)	2287.2	2071.0	546.9	215.2	123.4	133.8
	UB3LYP/cc-pVTZ (ω)	2408.2(85)	2239.4(121)	514.5(56)	157.8(11)	90.8(6)	94.6(0.4)
	Scaled ^d (ν)	2285.3	2148.7				
	Observed (ν)	2285.3	2148.7				
$^{14}\text{N}^{15}\text{N}^{12}\text{C}^{16}\text{O}^+$	UB3LYP/cc-pVTZ (ω)	2367.9(78)	2239.1(125)	510.6(57)	156.6(11)	89.4(5)	92.6(0.3)
	Scaled ^d (ν)	2247.1	2148.4				
	Observed (ν)	2247.3	2148.3				
$^{15}\text{N}^{14}\text{N}^{12}\text{C}^{16}\text{O}^+$	UB3LYP/cc-pVTZ (ω)	2368.3(78)	2239.0(126)	513.9(56)	156.7(11)	89.8(6)	93.5(0.5)
	Scaled ^d (ν)	2247.4	2148.3				
	Observed (ν)	2247.3	2148.3				
$^{15}\text{N}^{15}\text{N}^{12}\text{C}^{16}\text{O}^+$	UB3LYP/cc-pVTZ (ω)	2327.6(67)	2238.6(133)	510.0(57)	155.5(11)	88.4(5)	91.5(0.4)
	Scaled ^d (ν)	2208.8	2147.9				
	Observed (ν)	2210.1	2147.6				
$^{14}\text{N}^{14}\text{N}^{13}\text{C}^{16}\text{O}^+$	UB3LYP/cc-pVTZ (ω)	2407.9(89)	2190.2(108)	501.3(51)	156.9(10)	90.4(5)	94.6(0.4)
	Scaled ^d (ν)	2285.0	2101.5				
	Observed (ν)	2289.5 ^c	2102.2				
$^{14}\text{N}^{14}\text{N}^{12}\text{C}^{18}\text{O}^+$	UB3LYP/cc-pVTZ (ω)	2407.9(89)	2184.7(118)	512.2(57)	153.9(9)	90.5(6)	94.3(0.4)
	Scaled ^d (ν)	2285.0	2096.2				
	Observed (ν)	2286.5	2097.1				
$^{15}\text{N}^{15}\text{N}^{13}\text{C}^{16}\text{O}^+$	UB3LYP/cc-pVTZ (ω)	2326.8(77)	2189.8(114)	496.7(52)	154.7(11)	88.4(5)	92.1(0.4)
	Scaled ^d (ν)	2208.1	2101.3				
	Observed (ν)	2208.5	2101.9				

^aCalculated intensities (km/mol) are indicated in parentheses.

^bBased on previous investigations, the standard uncertainty (type B) in the neon-matrix measurements is 0.1 cm^{-1} (1σ).

^cReference 15.

^dScaling factors for ν_1 and ν_2 were chosen to make the calculated values for ν_1 and ν_2 of $^{14}\text{N}^{14}\text{N}^{12}\text{C}^{16}\text{O}^+$ equal the observed values. The scaling factor for ν_1 equals 0.94897, and that for ν_2 equals 0.95950.

^eVery weak and broad.

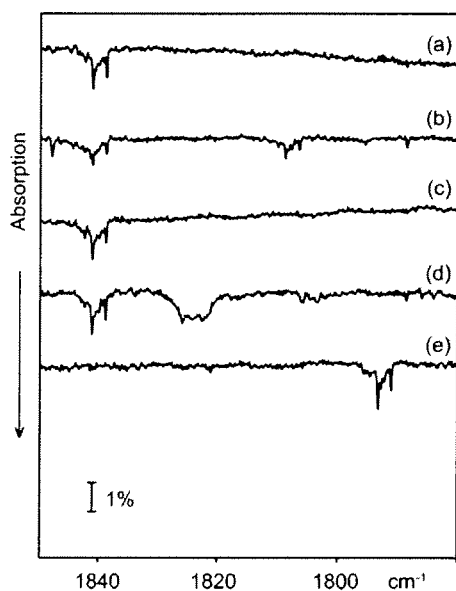


FIG. 7. Behavior of product absorptions between 1780 and 1850 cm^{-1} on isotopic enrichment of the same Ne: N_2 :CO samples as those for which spectra are shown in Figure 3.

values—0.94897 and 0.95950, respectively—are of the magnitude typical for similar scaling corrections. The agreement of the calculated and observed isotopologue frequencies given in Table II supports the assignment of the observed absorptions to NNCO^+ . The observed position for the CO-stretching fundamental, ν_2 , of NNCO^+ corresponds more closely to the value calculated in the density functional calculations than to the ν_2 value obtained by Hochlaf *et al.*,¹⁵ which is $\sim 75 \text{ cm}^{-1}$ too low. Possibly vibronic interactions with other low-lying electronic states of NNCO^+ , later discussed by Hochlaf,¹⁷ contribute to this disparity.

In the Ne: $^{14}\text{N}_2$: ^{13}CO (93%) study shown in Figures 3 and 4, trace (d), the other member of the Fermi resonance pair near 2285.3 cm^{-1} may have been shifted downward by more than the estimated 0.2 cm^{-1} , so that it is under the very sharp 2284.0 cm^{-1} edge of the prominent $^{13}\text{CO}_2$ absorption. The very weak, photosensitive absorption at 2289.5 cm^{-1} lies 187.3 cm^{-1} above the 2102.2 cm^{-1} ^{13}CO -stretching fundamental of the complex. The density functional calculations predict ω_4 near 157 cm^{-1} and ω_5 near 90 cm^{-1} for $^{14}\text{N}_2^{13}\text{CO}^+$. Either ν_4 or $2\nu_5$ could participate in the Fermi resonance interaction, with ν_4 somewhat more probable. As is shown in Table II, the values obtained for ν_4 and ω_4 in the calculations by Hochlaf *et al.*¹⁵ are 215.2 and 181.2 cm^{-1} , respectively. Since the position of ω_4 of $^{14}\text{N}_2^{13}\text{CO}^+$ is only 0.9 cm^{-1} lower than that obtained in the density functional calculations for the unenriched molecule, an estimate of 190 cm^{-1} for ν_4 of the unenriched species seems reasonable.

In the Ne: $^{15}\text{N}_2$ (97%): ^{13}CO (93%) study shown in Figures 5 and 6, trace (b), the photosensitive absorptions at 2208.5 and 2101.9 cm^{-1} are separated by 106.6 cm^{-1} . The density functional calculations summarized in Table II estimate that ω_4 and ω_5 of $^{15}\text{N}_2^{13}\text{CO}^+$ lie at 154.7 and 88.4 cm^{-1} , respectively. ω_6 is calculated to lie at 92.1 cm^{-1} , but, because of its a'' symmetry, it cannot participate in a Fermi

TABLE IV. Frequencies (cm^{-1}) observed for NO-stretching fundamental of NOCN isotopologues.

Species	Ne Matrix ^a		Ar matrix ^b	
	ν_{NO}	Shift	ν_{NO}	Shift
$^{14}\text{N}^{16}\text{O}^{12}\text{C}^{14}\text{N}$	1841.1		1836.9	
$^{14}\text{N}^{16}\text{O}^{13}\text{C}^{14}\text{N}$	1841.0	0.1	1836.9	0.0
$^{15}\text{N}^{16}\text{O}^{12}\text{C}^{14}\text{N}$	1808.7	32.4	1804.9	32.0
$^{14}\text{N}^{18}\text{O}^{12}\text{C}^{14}\text{N}$	1793.3	47.8	1789.2	47.7

^aThis work.

^bReference 3.

resonance with a fundamental of a' symmetry. ω_5 is a reasonable candidate for participation in the Fermi resonance interaction for $^{15}\text{N}_2^{13}\text{CO}^+$. From Table II, the density functional calculations predict that ω_5 of the unenriched species should lie near 90.8 cm^{-1} , 2.4 cm^{-1} higher than the value for the isotopologue under discussion. The RCCSD(T)/cc-pVTZ calculations of Hochlaf *et al.*¹⁵ predict values of 101.1 and 123.4 cm^{-1} for ω_5 and ν_5 , respectively, of unenriched NNCO^+ . The results of this comparison support a value near 110 cm^{-1} for ν_5 of NNCO^+ and its participation in the proposed Fermi resonance of $^{15}\text{N}_2^{13}\text{CO}^+$.

B. Carrier of the 1841.1 cm^{-1} absorption

The initial spectra of Ne: N_2 :CO samples which were codeposited with a beam of excited neon atoms also show a structured absorption at 1841.1 cm^{-1} which has a secondary maximum at 1838.7 cm^{-1} . This absorption, shown in trace (a) of Figure 7, is almost completely destroyed when the deposit is exposed to near infrared radiation of wavelength longer than 780 nm. The corresponding absorption patterns observed in the various isotopically enriched systems are shown in traces (b)–(e) of Figure 7.

Maier *et al.*³ assigned the infrared spectra of three of five relatively low energy products of the interaction of NO with CN, isolated in an argon matrix. The most prominent vibrational fundamental of NOCN was identified at 1836.9 cm^{-1} . The observed pattern of isotopic shifts indicated that this absorption is contributed by the stretching of the end NO-group. The end NC-stretching vibration contributed a very weak absorption at 2086.0 cm^{-1} . The other four fundamentals lie below 500 cm^{-1} . The positions and isotopic shifts observed for the NO-stretching absorption in our neon-matrix experiments are compared in Table IV with those observed in the argon-matrix study by the Maier group. The agreement is excellent and supports the earlier identifications.

IV. CONCLUSIONS

When a Ne: N_2 :CO = 200 mixture is codeposited at 4.3 K with a beam of neon atoms that have been excited in a microwave discharge, the infrared spectrum of the initial deposit includes new absorptions at 2285.3 and 2148.7 cm^{-1} that can be assigned to the NN- and CO-stretching fundamentals, respectively, of NNCO^+ . The positions observed for these absorptions are consistent with those obtained in previ-

ous high-level *ab initio* calculations and in the present density functional calculations. Isotopic substitution experiments have yielded the infrared spectra of seven isotopologues of NNCO⁺. The observed isotopic shifts for these vibrational fundamentals are consistent with those obtained in the density functional calculations. Perturbations of the NN-stretching absorptions of ¹⁴N₂¹³CO⁺ and ¹⁵N₂¹³CO⁺ are attributed to Fermi resonance interaction with a combination of the CO-stretching fundamental and a low-frequency deformation fundamental. The estimated values for two low-frequency fundamentals are consistent with the calculated positions of these two fundamentals. The previously identified NO-stretching fundamental of NOCN also appears in the spectra of the initial deposits. Its position and isotopic shifts support its earlier identification in an argon matrix.

ACKNOWLEDGMENTS

This paper is dedicated to Professor Helge Willner, University of Wuppertal, on the occasion of his 65th birthday.

- ¹P. Horsewood and G. W. Kirby, *J. Chem. Soc. D: Chem. Commun.* **1971**, 1139.
- ²R. Dickinson, G. W. Kirby, J. G. Sweeny, and J. K. Tyler, *J. Chem. Soc., Chem. Commun.* **1973**, 241.
- ³G. Maier, H. P. Reisenauer, J. Eckwert, M. Naumann, and M. De Marco, *Angew. Chem., Int. Ed. Engl.* **36**, 1707 (1997).
- ⁴A. A. Korkin, P. V. R. Schleyer, and R. J. Boyd, *Chem. Phys. Lett.* **227**, 312 (1994).
- ⁵G. de Petris, F. Cacace, R. Cipollini, A. Cartoni, M. Rosi, and A. Troiani, *Angew. Chem., Int. Ed.* **44**, 462 (2005).
- ⁶X. Zeng, H. Beckers, H. Willner, and J. F. Stanton, *Angew. Chem., Int. Ed.* **50**, 1720 (2011).
- ⁷A. Perrin, X. Zeng, H. Beckers, and H. Willner, *J. Mol. Spectrosc.* **269**, 30 (2011).
- ⁸C. E. Hamilton, V. M. Bierbaum, and S. R. Leone, *J. Chem. Phys.* **83**, 601 (1985).

- ⁹E. E. Ferguson, N. G. Adams, and D. Smith, *Chem. Phys. Lett.* **128**, 84 (1986).
- ¹⁰G. B. I. Scott, D. A. Fairley, C. G. Freeman, M. J. McEwan, and V. G. Anicich, *J. Chem. Phys.* **109**, 9010 (1998).
- ¹¹J. Glosik, G. Bano, E. E. Ferguson, and W. Lindinger, *Int. J. Mass Spectrom.* **176**, 177 (1998).
- ¹²W. Lu, P. Tosi, and D. Bassi, *J. Chem. Phys.* **113**, 4132 (2000).
- ¹³L. B. Knight, Jr., J. Steadman, P. K. Miller, and J. A. Cleveland, Jr., *J. Chem. Phys.* **88**, 2226 (1988).
- ¹⁴J. Baker and A. D. Buckingham, *J. Chem. Soc., Faraday Trans. 2* **83**, 1609 (1987).
- ¹⁵M. Hochlaf, C. Léonard, E. E. Ferguson, P. Rosmus, E.-A. Reinsch, S. Carter, and N. C. Handy, *J. Chem. Phys.* **111**, 4948 (1999).
- ¹⁶K. P. Huber and G. Herzberg, *Molecular Spectra and Molecular Structure. IV. Constants of Diatomic Molecules* (Van Nostrand Reinhold, New York, 1979).
- ¹⁷M. Hochlaf, *J. Phys. Chem. A* **108**, 4978 (2004).
- ¹⁸M. E. Jacox, *Chem. Soc. Rev.* **31**, 108 (2002).
- ¹⁹W. E. Thompson and M. E. Jacox, *J. Chem. Phys.* **93**, 3856 (1990).
- ²⁰W. E. Thompson and M. E. Jacox, *J. Chem. Phys.* **95**, 735 (1991).
- ²¹L. B. Knight, Jr., K. D. Johanneson, D. C. Cobranchi, E. A. Earl, D. Feller, and E. R. Davidson, *J. Chem. Phys.* **87**, 885 (1987).
- ²²L. B. Knight, Jr., J. Steadman, P. K. Miller, D. E. Bowman, E. R. Davidson, and D. Feller, *J. Chem. Phys.* **80**, 4593 (1984).
- ²³Certain commercial instruments and materials are identified in this paper in order to specify adequately the experimental procedure. In no case does such identification imply recommendation or endorsement by the National Institute of Standards and Technology, nor does it imply that the instruments or materials identified are necessarily the best available for the purpose.
- ²⁴M. E. Jacox and W. E. Thompson, *J. Chem. Phys.* **91**, 1410 (1989).
- ²⁵D. Forney, W. E. Thompson, and M. E. Jacox, *J. Chem. Phys.* **97**, 1664 (1992).
- ²⁶M. E. Jacox and W. B. Olson, *J. Chem. Phys.* **86**, 3134 (1987).
- ²⁷R. A. Toth, *J. Opt. Soc. Am. B* **8**, 2236 (1991).
- ²⁸R. A. Toth, *J. Opt. Soc. Am. B* **10**, 2006 (1993).
- ²⁹M. E. Jacox, in *Physics and Chemistry at Low Temperatures*, edited by L. Khriachtchev (Pan Stanford Publishing Pte. Ltd., Singapore, 2011), p. 1.
- ³⁰M. E. Jacox and W. E. Thompson, *J. Chem. Phys.* **123**, 064501 (2005).
- ³¹M. J. Frisch, G. W. Trucks, H. B. Schlegel *et al.*, GAUSSIAN 03, Revision B.01, Gaussian, Inc., Wallingford, CT, 2004.
- ³²A. D. Becke, *J. Chem. Phys.* **98**, 5648 (1993); C. Lee, W. Yang, and R. G. Parr, *Phys. Rev. B* **37**, 785 (1988).
- ³³T. H. Dunning, *J. Chem. Phys.* **90**, 1007 (1989).